Emergent SU(4) Symmetry in α-$ZrCl_3$ and Crystalline Spin-Orbital Liquids

Masahiko G. Yamada,[1,*] Masaki Oshikawa,[1] and George Jackeli[2,3,†]
[1]Institute for Solid State Physics, University of Tokyo, Kashiwa 277-8581, Japan
[2]Institute for Functional Matter and Quantum Technologies, University of Stuttgart, Pfaffenwaldring 57, D-70569 Stuttgart, Germany
[3]Max Planck Institute for Solid State Research, Heisenbergstrasse 1, D-70569 Stuttgart, Germany

(Received 3 October 2017; revised manuscript received 16 July 2018; published 27 August 2018)

While the enhancement of spin-space symmetry from the usual SU(2) to SU(N) is promising for finding nontrivial quantum spin liquids, its realization in magnetic materials remains challenging. Here, we propose a new mechanism by which SU(4) symmetry emerges in the strong spin-orbit coupling limit. In d^1 transition metal compounds with edge-sharing anion octahedra, the spin-orbit coupling gives rise to strongly bond-dependent and apparently SU(4)-breaking hopping between the $J_{\mathrm{eff}} = 3/2$ quartets. However, in the honeycomb structure, a gauge transformation maps the system to an SU(4)-symmetric Hubbard model. In the strong repulsion limit at quarter filling, as realized in α-$ZrCl_3$, the low-energy effective model is the SU(4) Heisenberg model on the honeycomb lattice, which cannot have a trivial gapped ground state and is expected to host a gapless spin-orbital liquid. By generalizing this model to other three-dimensional lattices, we also propose crystalline spin-orbital liquids protected by this emergent SU(4) symmetry and space group symmetries.

DOI: 10.1103/PhysRevLett.121.097201

Introduction.—Nontrivial quantum spin liquids (QSLs) are expected to exhibit many exotic properties such as fractionalized excitations [1,2], in addition to the absence of long-range order. Despite vigorous studies in the last several decades, however, material candidates for such QSLs are still rather limited.

An intriguing scenario to realize a nontrivial QSL is by generalizing the spin system, which usually consists of spins representing the SU(2) symmetry to SU(N) "spin" systems with $N > 2$. We expect stronger quantum fluctuations in SU(N) spin systems with a larger N, which could lead the system to an SU(N) QSL even on unfrustrated, bipartite lattices, including the honeycomb lattice [3–6].

The SU(N) spin systems with $N > 2$ can be realized in ultracold atomic systems, using the nuclear spin degrees of freedom (d.o.f.)[7]. In electron spin systems, however, realization of this SU(N) symmetry is more challenging. It would be possible to combine the spin and orbital d.o.f. so that local electronic states are identified with a representation of SU(N). QSL realized in this context may be called quantum spin-orbital liquids (QSOLs) because it involves spin and orbital d.o.f. Despite the appeal of such a possibility, the actual Hamiltonian is usually not SU(N)-symmetric, reflecting the different physical origins of the spin and orbital d.o.f. For example, the relevance of an SU(4) QSOL has been discussed for $Ba_3CuSb_2O_9$ (BCSO) with a decorated honeycomb lattice structure [5,8,9]. It turned out, however, that the estimated parameters for BCSO are rather far from the model with an exact SU(4) symmetry [10]. Moreover, the spin-orbit coupling (SOC) and the directional dependence of the orbital hopping usually break both the spin-space and orbital-space SU(2) symmetries, as exemplified in iridates [11]. Thus, it would seem even more difficult to realize an SU(N)-symmetric system in real magnets with SOC. (See Refs. [12–15] for the proposed realization of SU(N) symmetry. However, they do not lead to QSOL because of their crystal structures).

In this Letter, we demonstrate a novel mechanism for realizing an SU(4) spin system in a solid-state system with an on site SOC. Paradoxically, the symmetry of the spin-orbital space can be *enhanced* to SU(4) when the SOC is strong. In particular, we propose α-$ZrCl_3$ [16–18] as the first candidate for an SU(4)-symmetric QSOL on the honeycomb lattice. Its d^1 electronic configuration in the octahedral ligand field, combined with the strong SOC, implies that the ground state of the electron is described by a $J_{\mathrm{eff}} = 3/2$ quartet [19]. In fact, the resulting effective Hamiltonian appears to be anisotropic in the quartet space. Nevertheless, we show that the model is gauge equivalent to an SU(4)-symmetric Hubbard model. In the strong repulsion limit, its low-energy effective Hamiltonian is the Kugel-Khomskii model [20] on the honeycomb lattice, exactly at the SU(4) symmetric point,

$$H_{\mathrm{eff}} = J\sum_{\langle ij\rangle}\left(\boldsymbol{S}_i\cdot\boldsymbol{S}_j+\frac{1}{4}\right)\left(\boldsymbol{T}_i\cdot\boldsymbol{T}_j+\frac{1}{4}\right), \qquad (1)$$

where $J > 0$, and $\boldsymbol{S}_j$ and $\boldsymbol{T}_j$ are pseudospin-1/2 operators defined for each site j. SU(4) symmetry can be made manifest by rewriting the Hamiltonian, up to a constant

shift, as $H_{\rm eff} = (J/4)\sum_{\langle ij\rangle} P_{ij}$, where the spin state at each site forms the fundamental representation of SU(4), and P_{ij} is the operator which swaps the states at sites i and j. This is a natural generalization of the antiferromagnetic SU(2) Heisenberg model to SU(4).

The ground state of the SU(2) spin-1/2 antiferromagnet on the honeycomb lattice is simply Néel ordered [21,22], reflecting the unfrustrated nature of the lattice. On the other hand, the SU(N) generalization of the Néel state by putting different flavors on neighboring sites gives a macroscopic number of classical ground states when $N > 2$ [23–25], implying its instability. In fact, it was argued that the SU(4) antiferromagnet on the honeycomb lattice has a QSOL ground state without any long-range order [5,6].

Candidate materials.—As we mentioned in the Introduction, we propose α-$ZrCl_3$ with a honeycomb geometry as the first candidate for the d^1 honeycomb system, as shown in Fig. 1. More generally, we consider the class of materials α-MX_3, with M = Ti, Zr, Hf, etc. and X = F, Cl, Br, etc. Their crystal structure is almost the same as that of α-$RuCl_3$, which is known to be an approximate realization of the Kitaev honeycomb model [26,27]. However, the electronic structure of α-MX_3 is different from α-$RuCl_3$; here, M is in the 3+ state with a d^1 electronic configuration in the octahedral ligand field. Our strategy for the realization of SU(4) spin models starts with a low-energy quartet of electronic states with the effective angular momentum $J_{\rm eff} = 3/2$ on each M.

For this description to be valid, the SOC has to be strong enough. As the atomic number increases from Ti to Hf, SOC gets stronger, and the description by the effective angular momentum becomes exact. The compounds α-MCl_3 with M = Ti, Zr, and related Na_2VO_3 have been already reported experimentally. For α-$TiCl_3$, a structural transition and opening of the spin gap at $T = 217$ K have been reported [28]. This implies a small SOC, as is consistent with a massively degenerate manifold of spin singlets expected in the limit of a vanishing SOC [29]. In compounds with heavier elements, the strong SOC can convert this extensively degenerate manifold of product states into a resonating quantum state. Thus, we expect realization of the SU(4) QSOL due to strong SOC with metal ions heavier than Ti. In the following, we pick up α-$ZrCl_3$ as an example, although the same analysis should apply to α-$HfCl_3$ and $A_2M'O_3$ (A = Na, Li, etc., M' = Nb, Ta, etc.) as well.

Effective Hamiltonian.—In the strong ligand field, the description with one electron in the threefold degenerate t_{2g} shell for α-$ZrCl_3$ becomes exact. We denote these d_{yz}, d_{zx}, and d_{xy} orbitals by a, b, c, respectively. Let $a_{j\sigma}$, $b_{j\sigma}$, and $c_{j\sigma}$ represent annihilation operators on these orbitals on the jth site of Zr^{3+} with spin σ and $n_{\xi\sigma j}$ with $\xi \in \{a, b, c\}$ the corresponding number operators. We also use this $(a, b, c) = (yz, zx, xy)$ notation to label bonds; each Zr–Zr bond is called a ξ bond ($\xi = a, b, c$) when the superexchange pathway is on the ξ plane [30], as illustrated in Fig. 2.

We define a $J_{\rm eff} = 3/2$ quartet spinor as $\psi = (\psi_{\uparrow\uparrow}, \psi_{\uparrow\downarrow}, \psi_{\downarrow\uparrow}, \psi_{\downarrow\downarrow})^t = (\psi_{3/2}, \psi_{-3/2}, \psi_{1/2}, \psi_{-1/2})^t$, where ψ_{J^z} is the annihilation operator for the $|J = 3/2, J^z\rangle$ state. Assuming the SOC is the largest electronic energy scale, except for the ligand field splitting, fermionic operators can be rewritten by the quartet $\psi_{j\tau\sigma}$ as follows:

$$a^\dagger_{j\sigma} = \frac{\sigma}{\sqrt{6}}(\psi^\dagger_{j\uparrow\bar{\sigma}} - \sqrt{3}\psi^\dagger_{j\downarrow\sigma}), \tag{2}$$

$$b^\dagger_{j\sigma} = \frac{i}{\sqrt{6}}(\psi^\dagger_{j\uparrow\bar{\sigma}} + \sqrt{3}\psi^\dagger_{j\downarrow\sigma}), \tag{3}$$

$$c^\dagger_{j\sigma} = \sqrt{\frac{2}{3}}\psi^\dagger_{j\uparrow\sigma}, \tag{4}$$

where the indices τ and σ of $\psi_{j\tau\sigma}$ label the pseudoorbital and pseudospin indices, respectively. We begin from the following Hubbard Hamiltonian for α-$ZrCl_3$,

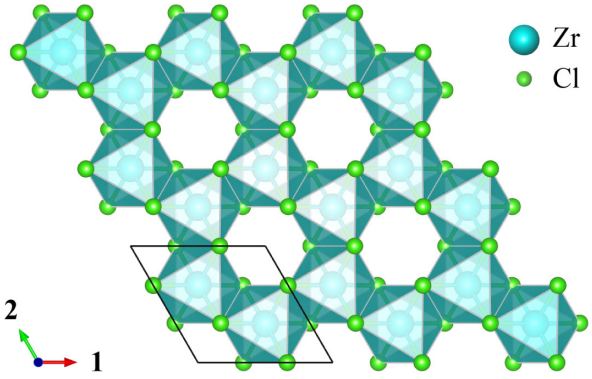

FIG. 1. Geometric structure of honeycomb α-$ZrCl_3$. Cyan and light green spheres represent Zr and Cl, respectively. The crystallographic axes are shown and labeled as the 1 and 2 directions.

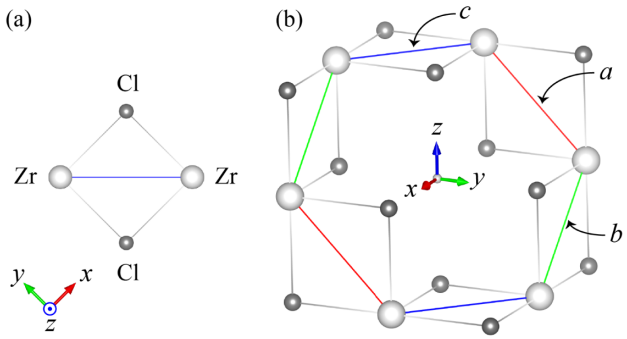

FIG. 2. (a) Superexchange pathways between two Zr ions connected by a c bond (blue) in α-$ZrCl_3$. White and gray spheres represent Zr and Cl atoms, respectively. (b) Three different types of bonds in α-$ZrCl_3$. Red, light green, and blue bonds represent a, b, and c bonds on the yz, zx, and xy planes, respectively.

$$H = -t \sum_{\sigma,\langle ij\rangle\in\alpha} (\beta^\dagger_{i\sigma}\gamma_{j\sigma} + \gamma^\dagger_{i\sigma}\beta_{j\sigma}) + \text{H.c.} + \frac{U}{2} \sum_{j,(\delta,\sigma)\neq(\delta',\sigma')} n_{\delta\sigma j} n_{\delta'\sigma' j}, \quad (5)$$

where t is a real-valued hopping parameter through the hopping shown in Fig. 2(a), $U > 0$ is the Hubbard interaction, $\langle ij\rangle \in \alpha$ means that the bond $\langle ij\rangle$ is an α bond, and $\langle \alpha, \beta, \gamma\rangle$ runs over every cyclic permutation of $\langle a, b, c\rangle$, and $\delta, \delta' \in \{a, b, c\}$. By inserting Eqs. (2)–(4), we get

$$H = -\frac{t}{\sqrt{3}} \sum_{\langle ij\rangle} \psi^\dagger_i U_{ij} \psi_j + \text{H.c.} + \frac{U}{2} \sum_j \psi^\dagger_j \psi_j (\psi^\dagger_j \psi_j - 1), \quad (6)$$

where ψ_j is the $J_{\text{eff}} = 3/2$ spinor on the jth site, and $U_{ij} = U_{ji}$ is a 4×4 matrix

$$U_{ij} = \begin{cases} U^a = \tau^y \otimes I_2 & (\langle ij\rangle \in a) \\ U^b = -\tau^x \otimes \sigma^z & (\langle ij\rangle \in b), \\ U^c = -\tau^x \otimes \sigma^y & (\langle ij\rangle \in c) \end{cases} \quad (7)$$

where I_m is the $m \times m$ identity matrix, while $\boldsymbol{\tau}$ and $\boldsymbol{\sigma}$ are Pauli matrices acting on the τ and σ indices of $\psi_{j\tau\sigma}$, respectively. We note that $U^{a,b,c}$ are unitary and Hermitian, and thus, $U_{ji} = U_{ij}{}^\dagger = U_{ij}$.

Now, we consider a (local) SU(4) gauge transformation,

$$\psi_j \to g_j \psi_j, \qquad U_{ij} \to g_i U_{ij} g^\dagger_j, \quad (8)$$

where g_j is an element of SU(4) defined for each site j. For every loop C on the lattice, the SU(4) flux defined by the product $\prod_{\langle ij\rangle\in C} U_{ij}$ is invariant under the gauge transformation.

Remarkably, for each elementary hexagonal loop (which we call plaquette) p in the honeycomb lattice with the coloring illustrated in Fig. 2(b),

$$\prod_{\langle ij\rangle\in p} U_{ij} = U^a U^b U^c U^a U^b U^c = (U^a U^b U^c)^2 = -I_4, \quad (9)$$

which corresponds to just an Abelian phase π. Since all the flux operators on the honeycomb lattice can be made of some product of these plaquettes, there is an SU(4) gauge transformation to reduce the model (6) to the π-flux Hubbard model H with global SU(4) symmetry, as proven in Sec. A of the Supplemental Material (SM) [31].

$$H = -\frac{t}{\sqrt{3}} \sum_{\langle ij\rangle} \eta_{ij} \psi^\dagger_i \psi_j + \text{H.c.} + \frac{U}{2} \sum_j \psi^\dagger_j \psi_j (\psi^\dagger_j \psi_j - 1), \quad (10)$$

where the definition of $\eta_{ij} = \pm 1$, arranged to insert a π flux inside each plaquette, is included in Sec. A of the SM [31].

At quarter filling, i.e., one electron per site, which is the case in α-$ZrCl_3$, the system becomes a Mott insulator for a sufficiently large $U/|t|$. The low-energy effective Hamiltonian for the spin and orbital d.o.f., obtained by the second-order perturbation theory in t/U, is the Kugel-Khomskii model exactly at the SU(4) point (1), with $\boldsymbol{S} = \boldsymbol{\sigma}/2$, $\boldsymbol{T} = \boldsymbol{\tau}/2$, and $J = 8t^2/(3U)$ in the transformed basis set. We note that the effective Hamiltonian does not depend on the phase factor η_{ij}, as it cancels out in the second-order perturbation in t/U. Corboz *et al.* argued that this SU(4) Heisenberg model on the honeycomb lattice hosts a gapless QSOL [5]. Therefore, we have found a possible realization of gapless QSOL in α-$ZrCl_3$ with an *emergent* SU(4) symmetry.

The nontrivial nature of this model may be understood in terms of the Lieb-Schultz-Mattis-Affleck (LSMA) theorem for the SU(N) spin systems [25,47–49], generalized to higher dimensions [47,50–53]. As a result, under SU(N) symmetry and translation symmetry, the ground state of the SU(N) spin system with n spins of the fundamental representation per unit cell cannot be unique, if there is a nonvanishing excitation gap and n/N is not an integer. This rules out a featureless Mott insulator phase, which is defined as a gapped phase with a unique ground state, namely, without any spontaneous symmetry breaking or topological order.

For the honeycomb lattice ($n = 2$), there is no LSMA constraint for an SU(2) spin system [54]. Nevertheless, for the SU(4) spin system we discuss in this Letter, a twofold ground-state degeneracy is required to open the gap. This suggests the stability of a gapless QSOL phase of the SU(4) Heisenberg model on the honeycomb lattice. Especially, assuming the π-flux Dirac spin-orbital liquid ansatz proposed in Ref. [5] is correct, a mass gap for the Dirac spectrum is forbidden unless the SU(4) or translation symmetry is broken. Detailed analysis based on the LSMA theorem will be discussed in a separate publication [55].

Other possible structures.—In addition to three-dimensional (3D) inorganic polymorphs [31], metal-organic frameworks (MOFs) with motifs listed in Fig. 3 are an interesting playground to explore a variety of SU(4) QSOLs. It was recently argued [56] that Kitaev spin liquids can be realized in MOFs by a mechanism similar to the one in iridates [11]. Since the present derivation of an emergent

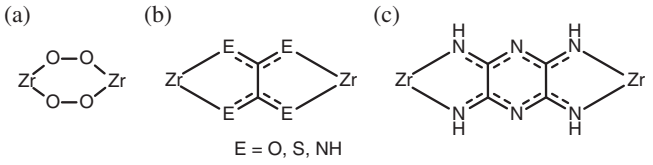

FIG. 3. Other possible superexchange pathways between two metal ions. (a) Zr–O–O–Zr. (b) Oxalate-based metal-organic motif. (E = O, S, NH.) (c) Tetraaminopyrazine-bridged metal-organic motif.

TABLE I. Tricoordinated lattices discussed in this Letter. Space groups are shown in number indices. Nonsymmorphic ones are underlined. n is the number of sites per unit cell.

Wells' notation	Lattice name	SU (4)	120° bond	n	Space group	LSMA
$(10,3)$-a	hyperoctagon	✓[a]	✓	4	**214**	✓[b]
$(10,3)$-b	hyperhoneycomb	✓[a]	✓	4	**70**	✓[b]
$(10,3)$-d		✓[a]		8	**52**	✓[b]
$(9,3)$-a	hypernonagon			12	**166**	
$8^2.10$-a		✓	✓	8	**141**	
$(8,3)$-b	hyperhexagon	✓	✓	6	**166**	✓[c]
	stripyhoneycomb	✓	✓	8	**66**	
(6,3)	2D honeycomb	✓	✓	2		✓[d]

[a]The product of hopping matrices along every elementary loop is unity, resulting in the SU(4) Hubbard model with zero flux.
[b]Nonsymmorphic symmetries of the lattice are enough to protect a QSOL state, i.e., hosting an XSOL state.
[c]Although the model has a π flux, with an appropriate gauge choice the unit cell is not enlarged. Therefore, the LSMA theorem straightforwardly applies to the π-flux SU(4) Hubbard model.
[d]While the standard LSMA theorem is not effective for the π-flux SU(4) Hubbard model here, the magnetic translation symmetry works to protect a QSOL state [62].

SU(4) symmetry shares the same t_{2g} hopping model as in Ref. [11], it is also expected to apply to Zr- or Hf-based MOFs. While Fig. 3(a) shows the longer superexchange pathways expected in oxides similar to triangular iridates [57], Figs. 3(b) and 3(c) show the superexchange pathways possible in Zr- or Hf-based MOFs. With these oxalate- or tetraaminopyrazine-based ligands, we can expect the two independent superexchange pathways similar to α-$ZrCl_3$ as discussed in Ref. [56].

Following the case of the honeycomb lattice, we can repeat the same analysis to derive the effective spin-orbital model for each 3D tricoordinated lattice. Recently, the classification of spin liquids on various tricoordinated lattices has attracted much attention, so it is worth investigating [58–60]. All the tricoordinated lattices considered in this Letter are listed in Table I. The table is based on the classification of tricoordinated nets by Wells [61]. We use a Schläfli symbol (p,c) to label a lattice, where p is the shortest elementary loop length of the lattice, and $c=3$ means the tricoordination of the vertices. For example, (6,3) is the two-dimensional (2D) honeycomb lattice, and all the other lattices are 3D tricoordinated lattices, distinguished by additional letters following Wells [61]. Here, $8^2.10$-a is a nonuniform lattice, and thus, the notation is different from the other lattices. Generalizing the discussion on the honeycomb lattice, if the SU(4) flux for any loop C is reduced to an Abelian phase ζ_C as $\prod_{\langle ij\rangle\in C} U_{ij} = \zeta_C I_4$ (for $^\forall C$), the Hubbard model acquires SU(4) symmetry. We have examined [31,55] this for each lattice in Table I, where a checkmark is put on the SU(4) column if the above condition holds. Moreover, in order to form a stable structure with the present mechanism, the bonds from each site must form 120 degrees and an octahedral coordination. This condition is again checked for each lattice and indicated in the 120° bond column [60] of Table I. We also put a checkmark on the LSMA column, when the LSMA theorem implies a ground state degeneracy or gapless excitations for the SU(4)-symmetric Hubbard model. For example, the LSMA constraint applies to the (8,3)-b lattice, since $n/N = 6/4$ is fractional.

Crystalline spin-orbital liquids.—Finally, we discuss the generalization of the concept of crystalline spin liquids (XSL) [63] to SU(4)-symmetric systems. In the context of gapless Kitaev spin liquids as proposed in Ref. [63], a crystalline spin liquid is defined as a spin liquid state where a gapless point (or a gapped topological phase) is protected not just by the unbroken time reversal or translation symmetry but by the space group symmetry of the lattice. In the (10,3) lattices listed in Table I, the unit cell consists of a multiple of four sites, and thus, the generalized LSMA theorem seems to allow a featureless insulator if we only consider the translation.

Following Refs. [64–66], however, we can effectively reduce the size of the unit cell by dividing the unit cell by the nonsymmorphic symmetry, and thus, the filling constraint becomes tighter with a nonsymmorphic space group. Even in the (10,3) lattices, the gapless QSOL state can be protected by the further extension of the LSMA theorem [55]. We call them crystalline spin-orbital liquids (XSOLs) in the sense that these exotic phases are protected in the presence of both SU(4) symmetry and (nonsymmorphic) space group symmetries. We put a checkmark on the LSMA column of Table I if either the standard or extended LSMA theorem applies.

Discussion.—We found that, as a consequence of the combination of the octahedral ligand field and SOC, SU(4) symmetry *emerges* in α-$ZrCl_3$. In addition to the $ZrCl_3$ (or $A_2M'O_3$ [31]) family we have discussed, Zr- or Hf-based MOFs could also realize SU(4) Heisenberg models on various tricoordinated lattices. Especially, 3D $(10,3)$-a [67], $(10,3)$-b [68], and $8^2.10$-a [63,69] lattices, as well as the 2D honeycomb lattice [70], were already realized in some MOFs with an oxalate ligand. Thus, we can expect that microscopic models defined by Eq. (5) on various tricoordinated lattices will apply in the same way as the honeycomb α-$ZrCl_3$ if we replace the metal ions of these MOFs with Zr^{3+}, Hf^{3+}, Nb^{4+}, or Ta^{4+} [56].

It would be also interesting to investigate SU(4) Heisenberg models on nontricoordinated lattices. Especially, on the lattice with 1 or 3 sites per unit cell, the LSMA theorem can exclude the possibility of a simply gapped $\mathbb{Z}_2$ spin liquid and suggests a $\mathbb{Z}_4$ QSOL or new symmetry-enriched topological phases instead.

Experimentally, muon spin resonance or nuclear magnetic resonance (NMR) experiments can rule out the existence of long-range magnetic ordering or spin freezing

in the spin sector. In the orbital sector, a possible experimental signature to observe the absence of orbital ordering or freezing should be finite-frequency electron spin resonance (ESR) [71] or extended X-ray absorption fine structure [9]. Especially, finite-frequency ESR can observe the dynamical Jahn-Teller (JT) effect [72,73], where the g-factor isotropy directly signals the quantum fluctuation between different orbitals [71,74,75]. This is applicable to our case because of the shape difference in the $J_{\mathrm{eff}} = 3/2$ orbitals [19], and the static JT distortion will result in the anisotropy in the in-plane g factors [76,77]. In addition, the specific heat or thermal transport measurements can distinguish between the gapped and gapless spectra. The emergent SU(4) symmetry would result in changing the universality class of critical phenomena or in the accidental coincidence between the timescales of two different excitations for spins and orbitals observed by NMR and ESR, respectively.

We thank A. Banisafar, K. Collins, K. Damle, E. Demler, V. Dwivedi, S. Ebihara, D. E. Freedman, Y. Fuji, B. I. Halperin, M. Hermanns, H. Katsura, G. Khaliullin, D. I. Khomskii, R. Kobayashi, M. Lajkó, L. Li, F. Mila, Y. Nakagawa, J. Romhanyi, R. Sano, K. Shtengel, A. Smerald, T. Soejima, H. Takagi, T. Takayama, T. Senthil, S. Tsuneyuki, and, especially, I. Kimchi for helpful comments. The crystal structure was taken from Materials Project. M. G. Y. is supported by the Materials Education program for the future leaders in Research, Industry, and Technology (MERIT) and by JSPS. This work was supported by JSPS KAKENHI Grants No. JP15H02113, No. JP17J05736, and No. JP18H03686, and by JSPS Strategic International Networks Program No. R2604 "TopoNet". We also acknowledge the support of the Max-Planck-UBC-UTokyo Centre for Quantum Materials. M. G. Y. acknowledges the Quantum Materials Department at MPI-FKF, Stuttgart for kind hospitality during his visits.

Note added.—Following the early version of the present paper on arXiv, a microscopic derivation of the SU(4) model on the hyperhoneycomb lattice has been reported [78].

*m.yamada@issp.u-tokyo.ac.jp
†Also at Andronikashvili Institute of Physics, 0177 Tbilisi, Georgia.

[1] L. Balents, Nature (London) **464**, 199 (2010).
[2] L. Savary and L. Balents, Rep. Prog. Phys. **80**, 016502 (2017).
[3] Y. Q. Li, M. Ma, D. N. Shi, and F. C. Zhang, Phys. Rev. Lett. **81**, 3527 (1998).
[4] M. Hermele and V. Gurarie, Phys. Rev. B **84**, 174441 (2011).
[5] P. Corboz, M. Lajkó, A. M. Läuchli, K. Penc, and F. Mila, Phys. Rev. X **2**, 041013 (2012).
[6] M. Lajkó and K. Penc, Phys. Rev. B **87**, 224428 (2013).
[7] M. Cazalilla and A. Rey, Rep. Prog. Phys. **77**, 124401 (2014).
[8] H. D. Zhou, E. S. Choi, G. Li, L. Balicas, C. R. Wiebe, Y. Qiu, J. R. D. Copley, and J. S. Gardner, Phys. Rev. Lett. **106**, 147204 (2011).
[9] S. Nakatsuji, K. Kuga, K. Kimura, R. Satake, N. Katayama, E. Nishibori, H. Sawa, R. Ishii, M. Hagiwara, F. Bridges, T. U. Ito, W. Higemoto, Y. Karaki, M. Halim, A. A. Nugroho, J. A. Rodriguez-Rivera, M. A. Green, and C. Broholm, Science **336**, 559 (2012).
[10] A. Smerald and F. Mila, Phys. Rev. B **90**, 094422 (2014).
[11] G. Jackeli and G. Khaliullin, Phys. Rev. Lett. **102**, 017205 (2009).
[12] F. J. Ohkawa, J. Phys. Soc. Jpn. **52**, 3897 (1983).
[13] R. Shiina, H. Shiba, and P. Thalmeier, J. Phys. Soc. Jpn. **66**, 1741 (1997).
[14] F. Wang and A. Vishwanath, Phys. Rev. B **80**, 064413 (2009).
[15] K. I. Kugel, D. I. Khomskii, A. O. Sboychakov, and S. V. Streltsov, Phys. Rev. B **91**, 155125 (2015).
[16] B. Swaroop and S. N. Flengas, Can. J. Chem. **42**, 1495 (1964).
[17] B. Swaroop and S. N. Flengas, Can. J. Phys. **42**, 1886 (1964).
[18] G. Brauer, *Handbuch der Präparativen Anorganischen Chemie, Bd. II* (Ferdinand Enke Verlag, Stuttgart, 1978).
[19] J. Romhányi, L. Balents, and G. Jackeli, Phys. Rev. Lett. **118**, 217202 (2017).
[20] K. I. Kugel and D. I. Khomskii, Sov. Phys. Usp. **25**, 231 (1982).
[21] J. D. Reger, J. A. Riera, and A. P. Young, J. Phys. Condens. Matter. **1**, 1855 (1989).
[22] J. Fouet, P. Sindzingre, and C. Lhuillier, Eur. Phys. J. B **20**, 241 (2001).
[23] M. Hermele, V. Gurarie, and A. M. Rey, Phys. Rev. Lett. **103**, 135301 (2009).
[24] A. V. Gorshkov, M. Hermele, V. Gurarie, C. Xu, P. S. Julienne, J. Ye, P. Zoller, E. Demler, M. D. Lukin, and A. M. Rey, Nat. Phys. **6**, 289 (2010).
[25] M. Lajkó, K. Wamer, F. Mila, and I. Affleck, Nucl. Phys. **B924**, 508 (2017).
[26] A. Kitaev, Ann. Phys. (Amsterdam) **321**, 2 (2006).
[27] K. W. Plumb, J. P. Clancy, L. J. Sandilands, V. V. Shankar, Y. F. Hu, K. S. Burch, H.-Y. Kee, and Y.-J. Kim, Phys. Rev. B **90**, 041112 (2014).
[28] S. Ogawa, J. Phys. Soc. Jpn. **15**, 1901 (1960).
[29] G. Jackeli and D. A. Ivanov, Phys. Rev. B **76**, 132407 (2007).
[30] The Cartesian xyz axes are defined as in Fig. 2(b).
[31] See Supplemental Material at http://link.aps.org/supplemental/10.1103/PhysRevLett.121.097201 for more details, which include Refs. [32–46].
[32] D. P. Arovas and A. Auerbach, Phys. Rev. B **52**, 10114 (1995).
[33] S. K. Pati, R. R. P. Singh, and D. I. Khomskii, Phys. Rev. Lett. **81**, 5406 (1998).
[34] C. Itoi, S. Qin, and I. Affleck, Phys. Rev. B **61**, 6747 (2000).

[35] X. Chen, Z.-C. Gu, and X.-G. Wen, Phys. Rev. B **83**, 035107 (2011).
[36] J. A. Watts, Inorg. Chem. **5**, 281 (1966).
[37] W. Rüdorff, G. Walter, and H. Becker, Z. Anorg. Allg. Chem. **285**, 287 (1956).
[38] T. Takayama, A. Kato, R. Dinnebier, J. Nuss, H. Kono, L. S. I. Veiga, G. Fabbris, D. Haskel, and H. Takagi, Phys. Rev. Lett. **114**, 077202 (2015).
[39] K. A. Modic, T. E. Smidt, I. Kimchi, N. P. Breznay, A. Biffin, S. Choi, R. D. Johnson, R. Coldea, P. Watkins-Curry, G. T. McCandless, J. Y. Chan, F. Gandara, Z. Islam, A. Vishwanath, A. Shekhter, R. D. McDonald, and J. G. Analytis, Nat. Commun. **5**, 4203 (2014).
[40] S. M. Winter, Y. Li, H. O. Jeschke, and R. Valentí, Phys. Rev. B **93**, 214431 (2016).
[41] C. Wu, J.-p. Hu, and S.-c. Zhang, Phys. Rev. Lett. **91**, 186402 (2003).
[42] C. Wu, Phys. Rev. Lett. **95**, 266404 (2005).
[43] C. Wu, Mod. Phys. Lett. B **20**, 1707 (2006).
[44] A. Georges, L. de' Medici, and J. Mravlje, Annu. Rev. Condens. Matter Phys. **4**, 137 (2013).
[45] O. Delgado Friedrichs, M. O'Keeffe, and O. M. Yaghi, Acta Crystallogr. Sect. A **59**, 22 (2003).
[46] O. Delgado Friedrichs, M. O'Keeffe, and O. M. Yaghi, Acta Crystallogr. Sect. A **59**, 515 (2003).
[47] E. Lieb, T. Schultz, and D. Mattis, Ann. Phys. (N.Y.) **16**, 407 (1961).
[48] I. Affleck and E. H. Lieb, Lett. Math. Phys. **12**, 57 (1986).
[49] Y. Yao, C.-T. Hsieh, and M. Oshikawa, arXiv:1805.06885.
[50] I. Affleck, Phys. Rev. B **37**, 5186 (1988).
[51] M. Oshikawa, Phys. Rev. Lett. **84**, 1535 (2000).
[52] M. B. Hastings, Europhys. Lett. **70**, 824 (2005).
[53] K. Totsuka, *JPS 72nd Annual Meeting, Osaka, Japan, 2017*.
[54] C.-M. Jian and M. Zaletel, Phys. Rev. B **93**, 035114 (2016).
[55] M. G. Yamada, M. Oshikawa, and G. Jackeli (to be published).
[56] M. G. Yamada, H. Fujita, and M. Oshikawa, Phys. Rev. Lett. **119**, 057202 (2017).
[57] A. Catuneanu, J. G. Rau, H.-S. Kim, and H.-Y. Kee, Phys. Rev. B **92**, 165108 (2015).
[58] M. Hermanns, K. O'Brien, and S. Trebst, Phys. Rev. Lett. **114**, 157202 (2015).
[59] M. Hermanns, S. Trebst, and A. Rosch, Phys. Rev. Lett. **115**, 177205 (2015).
[60] K. O'Brien, M. Hermanns, and S. Trebst, Phys. Rev. B **93**, 085101 (2016).
[61] A. F. Wells, *Three-Dimensional Nets and Polyhedra* (Wiley, New York, 1977).
[62] Y.-M. Lu, Y. Ran, and M. Oshikawa, arXiv:1705.09298.
[63] M. G. Yamada, V. Dwivedi, and M. Hermanns, Phys. Rev. B **96**, 155107 (2017).
[64] S. A. Parameswaran, A. M. Turner, D. P. Arovas, and A. Vishwanath, Nat. Phys. **9**, 299 (2013).
[65] H. Watanabe, H. C. Po, A. Vishwanath, and M. Zaletel, Proc. Natl. Acad. Sci. U.S.A. **112**, 14551 (2015).
[66] H. C. Po, H. Watanabe, C.-M. Jian, and M. P. Zaletel, Phys. Rev. Lett. **119**, 127202 (2017).
[67] E. Coronado, J. R. Galán-Mascarós, C. J. Gómez-García, and J. M. Martínez-Agudo, Inorg. Chem. **40**, 113 (2001).
[68] B. Zhang, Y. Zhang, and D. Zhu, Dalton Trans. **41**, 8509 (2012).
[69] M. Clemente-León, E. Coronado, and M. López-Jordà, Dalton Trans. **42**, 5100 (2013).
[70] B. Zhang, Y. Zhang, Z. Wang, D. Wang, P. J. Baker, F. L. Pratt, and D. Zhu, Sci. Rep. **4**, 6451 (2014).
[71] Y. Han, M. Hagiwara, T. Nakano, Y. Nozue, K. Kimura, M. Halim, and S. Nakatsuji, Phys. Rev. B **92**, 180410 (2015).
[72] J. Nasu and S. Ishihara, Phys. Rev. B **88**, 094408 (2013).
[73] J. Nasu and S. Ishihara, Phys. Rev. B **91**, 045117 (2015).
[74] I. Bersuker, Coord. Chem. Rev. **14**, 357 (1975).
[75] A. Abragam and B. Bleaney, *Electron Paramagnetic Resonance of Transition Ions* (Clarendon Press, Oxford, 1970).
[76] N. Iwahara, V. Vieru, L. Ungur, and L. F. Chibotaru, Phys. Rev. B **96**, 064416 (2017).
[77] We note that the trigonal distortion existing *a priori* in real materials only splits the degeneracy between the out-of-plane and in-plane g factors, and the splitting of the two in-plane modes clearly indicates an additional (e.g., tetragonal) distortion.
[78] W. M. H. Natori, E. C. Andrade, and R. G. Pereira, arXiv:1802.00044.